Zeolites

DOI: 10.1002/anie.200604336

Space- and Time-Resolved Visualization of Acid Catalysis in ZSM-5 Crystals by Fluorescence Microscopy**

*Maarten B. J. Roeffaers, Bert F. Sels, Hiroshi Uji-i, Bart Blanpain, Pieter L'hoëst, Pierre A. Jacobs, Frans C. De Schryver, Johan Hofkens, and Dirk E. De Vos**

Since their discovery in the 1970s, zeolites with MFI topology, such as ZSM-5 and silicalite, have been used for large-scale separation and catalytic processes.[1] While the crystallographic structure of ZSM-5 is sufficiently known, zeolites seldom occur as perfect single crystals. Large MFI crystals often have the "classic-boat" or "coffin" shape, and various approaches have been followed to demonstrate that such crystals contain either two or three pairs of components with different crystallographic orientation or properties.[2–5] The orientation of the components, access to the straight or sinusoidal channels, and the role of the interfaces between the components have been studied by various techniques, but for a deeper understanding, physicochemical techniques with improved temporal and particularly spatial resolution are required.

Few techniques are able to spatially map dynamic phenomena in micrometer-sized zeolite crystals, and in such studies, focus is generally on diffusion rather than on catalysis. Infrared microscopy allows observation of diffusion of arenes in zeolites, but with a limited spatial resolution.[6] By using interference microscopy, concentration gradients throughout silicalite crystals on sorption of small molecules have been mapped, and evidence for internal diffusion barriers has been found.[7] The diffusion of "preformed" dye molecules in porous materials has been followed by fluorescence microscopy at the single-molecule level[8] and for ensembles of molecules.[9] Finally, coke formation can be mapped by SEM-EDX analysis,[10] but from these ex situ measurements, little information is obtained on the dynamics or on the molecular nature of the species formed.

While most previous studies focus on diffusion, in situ visualization of a zeolite-catalyzed reaction has not yet been achieved. A reaction not only requires diffusion but also the availability of active sites. Moreover, a suitable analytical technique should distinguish between reagent and product molecules.[11] We here demonstrate that fluorescence microscopy can monitor catalytic, condensed-phase reactions in individual zeolite crystals. Spatially inhomogeneous product formation is observed as a function of time, and this gives insight into the relations between the crystal structure and reactivity.

Samples of Al-ZSM-5 were prepared by hydrothermal synthesis from gels containing tetrapropylammonium ions as template.[12] Optical transmission images show elongated crystals with typical width and height between 15 and 20 μm, and length between 75 and 90 μm. Samples were carefully calcined to avoid formation of defects such as cracks. The absence of major defects was confirmed by optical and scanning electron microscopy. Hourglass patterns are easily recognized under the optical microscope; at least two distinct models have been proposed to explain these patterns (Figure 1). In the first model, supported by X-ray precession photographs,[3] the coffin-shaped crystal is a 90° intergrowth of a central component and two pyramidal components; the crystallographic orientation of the latter is rotated by 90° around the [001] axis (Figure 1A).[2,3] In the second model, the crystal contains three pairs of components (Figure 1B); the crystallographic orientation is the same in the whole crystallite, but the concentration of MEL-type defects in each segment is different.[4,5] This model is based on the observation of a terrace structure of the (100) and (010) faces of silicalite samples by atomic force microscopy.[5] Terrace formation is related to incorporation of defects in the structure.

With well-characterized ZSM-5 crystallites in hand, catalytic test reactions were selected for the in situ study of electrophilic aromatic substitutions, such as the hydroxyalkylation of anisole or the self-condensation of furfuryl alcohol (**1**; Scheme 1). The acid-catalyzed reaction of two furfuryl alcohol molecules initially produces a colorless bis-(furyl)methyl group, as in **2**. This molecule easily transfers a hydride ion to a primary carbenium ion formed from another molecule of furfuryl alcohol. Visible absorption then arises

[*] M. B. J. Roeffaers, Prof. B. F. Sels, Prof. P. A. Jacobs, Prof. D. E. De Vos
Department of Microbial and Molecular Systems
Centre for Surface Chemistry and Catalysis
Katholieke Universiteit Leuven
Kasteelpark Arenberg 23, 3001 Leuven (Belgium)
Fax: (+32) 16-321-998
E-mail: dirk.devos@biw.kuleuven.be
Dr. H. Uji-i, Prof. F. C. De Schryver, Prof. J. Hofkens
Department of Chemistry
Katholieke Universiteit Leuven
Celestijnenlaan 200F, 3001 Leuven (Belgium)
Prof. B. Blanpain, P. L'hoëst
Department of Metallurgy and Materials Engineering
Katholieke Universiteit Leuven
Kasteelpark Arenberg 44, 3001 Leuven (Belgium)

[**] M.B.J.R. thanks the Institute for the Promotion of Innovation through Science and Technology in Flanders (IWT-Vlaanderen) for a fellowship. This work was performed within the framework of the IAP-V-03 programme "Supramolecular Chemistry and Catalysis" of the Belgian Federal government and of GOA-2/01. We also gratefully acknowledge support from the K.U. Leuven in the frame of the Centre of Excellence CECAT. We are grateful to G. Vanbutsele for a ZSM-5 sample.

Supporting information for this article is available on the WWW under http://www.angewandte.org or from the author.

InterScience DISCOVER SOMETHING GREAT
© 2007 Wiley-VCH Verlag GmbH & Co. KGaA, Weinheim

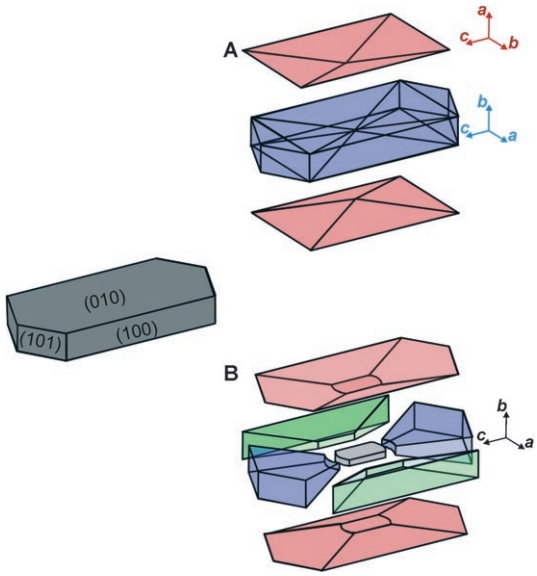

Figure 1. Internal structure of coffin-shaped MFI crystals.[2–5] A) Two-component model and B) three-component model.

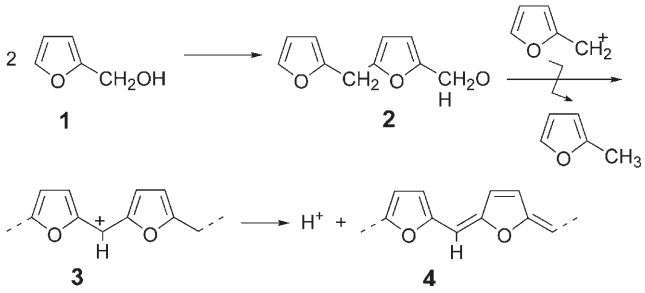

Scheme 1. Formation of chromophores in **3** and **4** during self-condensation of furfuryl alcohol.

from resonance-stabilized bis-furyl carbenium ion **3** or from conjugated structure **4** that is formed by proton loss.[13] On excitation with visible light, no emission is expected for reagent **1** or intermediate **2**, but compounds **3** and **4**, as well as their analogues, are fluorescent. As the degree of oligomerization and conjugation increase, the absorption and emission wavelengths of the chromophores shift towards the red.

Exposure of calcined, coffin-shaped ZSM-5 crystals to a solution of furfuryl alcohol in dioxane was monitored under the fluorescence microscope as a function of time. The first fluorescence arises at the (100) and (010) faces. Clearly, for a crystal lying on the (010) face, the optical path runs along the (100) face, and the accumulated fluorescence on this face causes the bright rim in Figure 2 A. Analogous phenomena

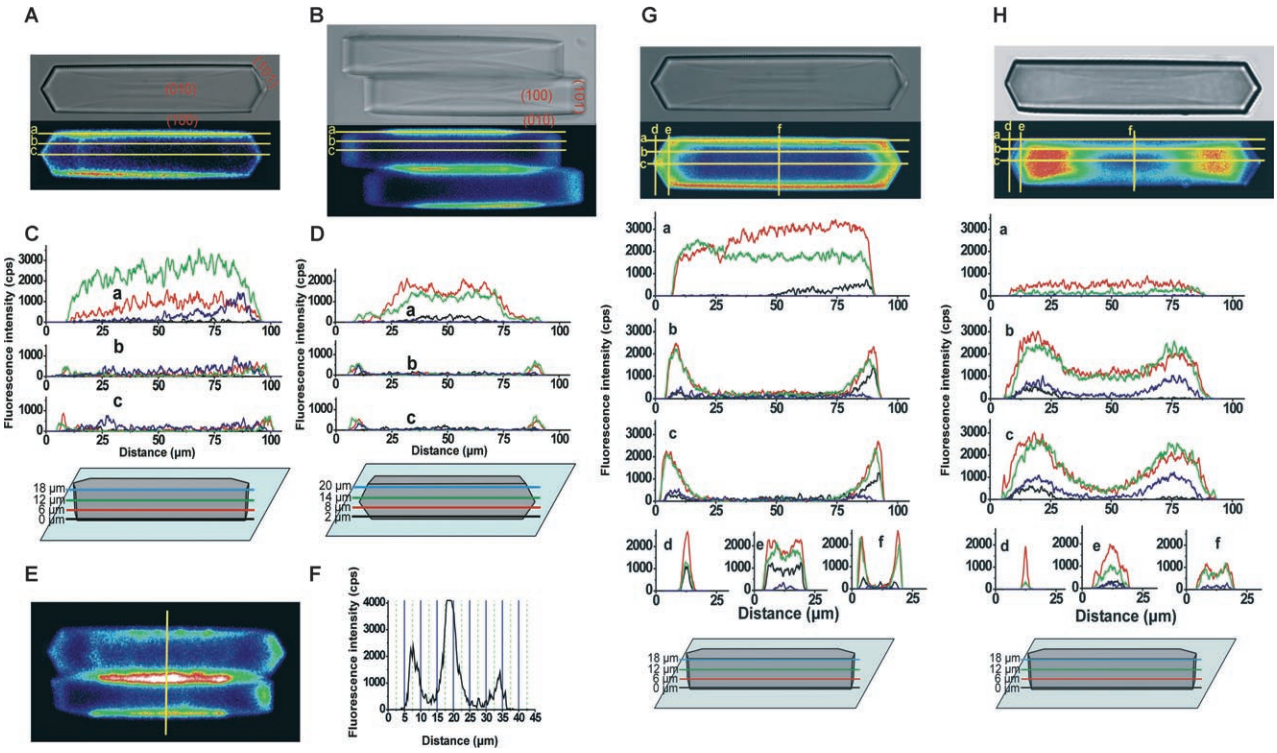

Figure 2. Confocal microscopic imaging of the condensation of furfuryl alcohol catalyzed by individual ZSM-5 zeolite crystals. A, B) Fluorescence intensity in ZSM-5 crystals after 10 min of reaction (false color, photomultiplier-tube (PMT) voltage 700 V), and corresponding optical transmission images (grayscale). Initial activity is located at the (100) and (010) faces. C) The fluorescence intensity along selected lines in (A) measured at various depths (black line at 0, red line at 6, green line at 12, and blue line at 18 μm from the cover glass; further lines omitted for clarity). D) Same plot for B (black line at 2, red line at 8, green line at 14, and blue line at 20 μm from the coverglass). E, F) For two crystals lying on (100) and (010), the intensity profile perpendicular to the *c* direction (in F) clearly shows the penetration of fluorescence from the outer surface into the interior of the crystal (selected line intensity in the crystal at 10 μm from the cover glass; reaction time 8 h). G) after 16 h reaction time, the slower reaction from the (101) and (10$\bar{1}$) faces has started (black line at 0, red line at 6, green line at 12, and blue line at 18 μm from the cover glass); PMT voltage: 600 V. H) after 50 days, intensity accumulates in the tips below (101) and (10$\bar{1}$); PMT voltage: 550 V. Colors in (A), (B), (G), and (H) cannot be compared directly because of different detector settings.

 © 2007 Wiley-VCH Verlag GmbH & Co. KGaA, Weinheim

are observed when the crystal is rotated by 90° around the *c* axis (Figure 2B), with a similar preference for the central zone of the (010) face. The spatial resolution is sufficient to follow the fluorescence intensity at any point in the crystal, for instance, by scanning through the crystal along the *c* direction at different distances from the crystal face, or at different depths *z* in the light path of the microscope (Figure 2C and D). In this early stage of the reaction, intensities are comparable on the (100) and (010) faces. Much less fluorescence is observed on the (101) and (10$\bar{1}$) faces.

Fluorescence microscopy not only gives space-resolved information; its time resolution also allows dynamic phenomena to be filmed. Thus, after initiation of the reaction, fluorescence gradually spreads into the crystal starting from (100) or (010). Figure 2E shows two adjacent crystals, lying on (010) and (100), in which product-related emission produces bright zones, next to darker zones which assume the well-recognizable hourglass shape. A line scan along the short *a* or *b* axis of the crystals reveals that the intensity peaks at the crystal borders are asymmetrical, that is, there is a gradient of product concentration into the interior of the crystal (Figure 2F). Such observations show that the pores at (100) and (010) are readily accessible. Moreover, there is no evidence that major cracks in the crystal or the interfaces along the hourglass pattern are the principal avenues for reagent uptake. The similar behavior of (100) and (010) faces implies that furfuryl alcohol does not distinguish between these faces when entering the ZSM-5 crystal. This could be in line with the first model (Figure 1A), in which both (100) and (010) faces give access to the sinusoidal pores. Alternatively, furfuryl alcohol may not be able to distinguish between the pore entrances of straight and sinusoidal channels, and the second model therefore cannot be discarded.

Clearly, the (101) and (10$\bar{1}$) faces, and the crystal components behind them (henceforward called "tips", see the blue components in Figure 1B) show a slower buildup of fluorescent products (Figure 2A and B). This supports the idea that the tips constitute separate segments within the crystal, besides the pyramidal segments swept out by (010) and (100). Two effects could lead to spatially inhomogeneous product formation: first, the concentration of active sites could be lower; second, access to these tip segments could be slower. To test the first hypothesis, spatially resolved elemental analyses were performed on an Al-ZSM-5 crystal by electron microprobe analysis (see the Supporting Information). Compositional gradients are easily recognized, with rather uniform Al enrichment at the crystal exterior. However, there is no evidence for Al depletion in the tip segments, which refutes the first hypothesis. Thus, it seems that direct reagent diffusion into the tip segments is difficult and causes lower reaction rates. Access from the (101) and (10$\bar{1}$) faces is expected to be quite slow, since molecules have to follow a tortuous path to diffuse along the *c* axis, by alternatingly employing straight and sinusoidal channels. The alternative access to the tip segments crosses the interfaces between the crystal components. Various roles have been attributed to these interfaces with regard to diffusion inside MFI crystals. It has been advocated that voids between the components provide easy access to the interior of the crystal, and to the straight channels in particular.[14] However, quantitative analysis of isobutane adsorption by interference microscopy is consistent with the interfaces' functioning as mild barriers for intracrystalline diffusion.[7] The low initial fluorescence intensity in the tip segments seems to be in clear agreement with the latter hypothesis.

At an intermediate stage of the reaction, fluorescence also spreads along the *c* axis into the tip segments, as illustrated by the longitudinal scans in Figure 2G. It seems that any zone in the crystal can be reached by the reagents. Surprisingly, a reversed situation is observed on prolonged exposure of the catalyst to the reagents: eventually, the tip segments emit the most intense fluorescence (Figure 2H). At such long reaction times, microporous zeolite catalysts tend to be deactivated by pore plugging. Clearly, desorption of the product molecules from the tip segments is slow and gives rise to extensive consecutive reactions such as oligomerization. This again is in line with the interfaces' functioning as diffusion barriers that impede fast product evacuation from the tip segments via the pyramidal segments to the exterior. Such buildup is much less observed in the pyramidal segments, which proves more efficient product evacuation via the (100) and (010) faces. The emissive plumes spread from the (101) and (10$\bar{1}$) facets into the crystal, and this identifies the tortuous path along the *c* direction as the principal route for reagent supply (Figure 2G).

A unique feature of fluorescence microscopy is not only its ability to detect product molecules against a reagent background, but also to selectively visualize products by selective excitation.[11] For instance, blue excitation at 488 nm of the aged crystal in Figure 3A reveals rather homogeneous emission from the whole crystal, but the emission after green excitation (543 nm) and particularly red excitation (633 nm) shows that the larger, more conjugated oligomeric products are indeed accumulated in the tips (Figure 3B–D).

In summary, the data show that the compartmentalization of coffin-shaped ZSM-5 crystals, as proposed in crystallographic studies, is also relevant to catalysis. The distinct behavior of the tip segments supports models that divide the

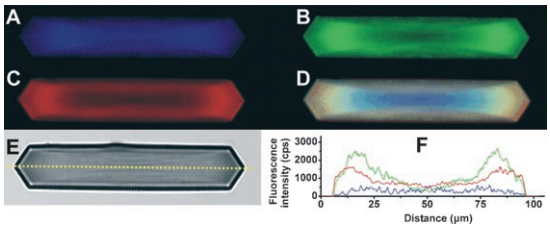

Figure 3. Multicolor imaging of reaction products from furfuryl alcohol after 50 days. A) In the blue channel (excitation at 488, detection between 505 and 560 nm), intense fluorescence is detected in the central part of the crystal. B) In the green channel (excitation at 543, detection between 560 and 660 nm) fluorescence appears in a domain closer to the outer surface of the crystal. C) The longest oligomers, which are visualized in the red channel (excitation at 633, detection from 660 nm) can be found at the extremities of the crystal, in the "tips" under the (101) and (10$\bar{1}$) faces. D) Overlay image of the three channels. E, F) A line scan along the *c* axis shows the relative intensities in the channels (averaged along the *z* direction). The three channels were recorded with the same PMT settings (600 V).

 © 2007 Wiley-VCH Verlag GmbH & Co. KGaA, Weinheim

crystals into three pairs of components (Figure 1B). More importantly, the interfaces between the components act as diffusion barriers, either for reagent adsorption or for product desorption. With other acid-catalyzed test reactions, such as hydroxyalkylation of anisole and dehydration of 1,3-diphenyl-1,3-propanediol,[15] analogous phenomena were observed.

While the above observations hold for at least 90% of the 150 studied crystals in the powdered sample, looking at individual crystals identifies unusual or exceptional behavior. A few crystals tend to accumulate intense fluorescence on the (101) and (10$\bar{1}$) facets, or alternatively, on small triangular parts of the (010) face close to the crystal end. Figure 4A and B show that the intense emission is confined to the outer surface. For such individual crystallites, unusual Al zoning could be the origin of these observations, even though the elemental analysis of typical crystals does not reveal anomalies.

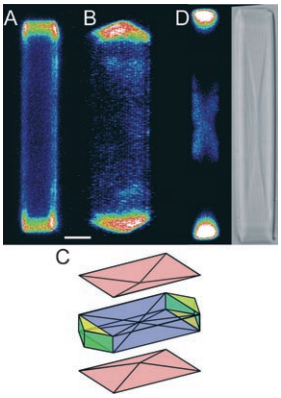

Figure 4. Exceptions in the crystal population. Crystals with pronounced activity on the (101) and (10$\bar{1}$) faces (A; indicated by green in the model in C) and on small triangular parts of the (010) face (B; indicated by yellow in C). Image B is a computer-generated view of the crystal in A, rotated by 90° around *c*. D) In another case a central cross can be seen, the location of which corresponds to the interfaces in the crystal. Scale bar: 10 μm.

Finally, the main results support the idea of internal interfaces functioning as diffusion barriers. However, a cross-shaped fluorescent feature unexpectedly appears in Figure 4D. The only rational explanation is that the crystal components have lost contact[16] and larger voids have been formed between them. Such voids are then a preferred route for penetration into the crystal. Variations in calcination could well cause such crystal damage.

In conclusion, we have demonstrated that fluorescence microscopy allows rapid three-dimensional and time-dependent mapping of catalytic activity in individual zeolite crystals. The reactivity of the various crystal domains can be followed throughout the lifetime of the catalyst.

Experimental Section

Fluorescence intensity and transmission images of the crystals were acquired with an IX70 Olympus microscope and the Fluoview FV500 operating system (Olympus; see the Supporting Information).

The catalytic reactions were performed in a liquid cell[17] in which the reagent, for example furfuryl alcohol, can be added to the dioxane solvent. The final substrate concentration was 10 vol%. All reactions were performed at room temperature.

Received: October 23, 2006
Published online: January 23, 2007

Keywords: crystal intergrowth · fluorescence microscopy · fluorescence spectroscopy · heterogeneous catalysis · zeolites

[1] *Zeolites for Cleaner Technologies* (Eds.: M. Guisnet, J.-P. Gilson), Imperial College Press, River Edge, NJ, **2002**.
[2] J. Caro, M. Noack, J. Richter-Mendau, F. Marlow, D. Petersohn, M. Griepentrog, J. Kornatowski, *J. Phys. Chem.* **1993**, *97*, 13685–13690.
[3] C. Weidenthaler, R. Fischer, R. Shannon, O. Medenbach, *J. Phys. Chem.* **1994**, *98*, 12687–12694.
[4] E. Geus, J. Jansen, H. van Bekkum, *Zeolites* **1994**, *14*, 82–88.
[5] J. Agger, N. Hanif, C. Cundy, A. Wade, S. Dennison, P. Rawlinson, M. Anderson, *J. Am. Chem. Soc.* **2003**, *125*, 830–839.
[6] a) E. Lehmann, C. Chmelik, H. Scheidt, S. Vasenkov, B. Staudte, J. Kärger, F. Kremer, G. Zadrozna, J. Kornatowski, *J. Am. Chem. Soc.* **2002**, *124*, 8690–8692; b) Y. S. Lin, N. Yamamoto, Y. Choi, T. Yamaguchi, T. Okubo, S.-I. Nakao, *Microporous Mesoporous Mater.* **2000**, *38*, 207–220.
[7] a) O. Geier, S. Vasenkov, E. Lehmann, J. Kärger, U. Schemmert, R. Rakoczy, J. Weitkamp, *J. Phys. Chem. B* **2001**, *105*, 10217–10222; b) J. Kärger, P. Kortunov, S. Vasenkov, L. Heinke, D. B. Shah, R. A. Rakoczy, Y. Traa, J. Weitkamp, *Angew. Chem.* **2006**, *118*, 8010–8013; *Angew. Chem. Int. Ed.* **2006**, *45*, 7846–7849.
[8] a) C. Hellriegel, J. Kirstein, C. Bräuchle, V. Latour, T. Pigot, R. Olivier, S. Lacombe, R. Brown, V. Guieu, C. Payrastre, A. Izquierdo, P. Mocho, *J. Phys. Chem. B* **2004**, *108*, 14699–14709; b) C. Hellriegel, J. Kirstein, C. Bräuchle, *New J. Phys.* **2005**, *7*, 23.
[9] a) G. Calzaferri, S. Huber, H. Maas, C. Minkowski, *Angew. Chem.* **2003**, *115*, 3860–3888; *Angew. Chem. Int. Ed.* **2003**, *42*, 3732–3758; b) C. Minkowski, G. Calzaferri, *Angew. Chem.* **2005**, *117*, 5459–5463; *Angew. Chem. Int. Ed.* **2005**, *44*, 5325–5329; c) A. Ruiz, H. Li, G. Calzaferri, *Angew. Chem.* **2006**, *118*, 5408–5413; *Angew. Chem. Int. Ed.* **2006**, *45*, 5282–5287.
[10] S. van Donk, J. Bitter, A. Verberckmoes, M. Versluijs-Helder, A. Broersma, K. de Jong, *Angew. Chem.* **2005**, *117*, 1384–1387; *Angew. Chem. Int. Ed.* **2005**, *44*, 1360–1363.
[11] M. Roeffaers, B. Sels, H. Uji-i, F. De Schryver, P. Jacobs, D. De Vos, J. Hofkens, *Nature* **2006**, *439*, 572–575.
[12] U. Mueller, K. Unger, *Zeolites* **1988**, *8*, 154–156.
[13] M. Choura, N. Belgacem, A. Gandini, *Macromolecules* **1996**, *29*, 3839–3850.
[14] M. Kocirik, J. Kornatowski, V. Masarik, P. Novak, A. Zikanova, J. Maixner, *Microporous Mesoporous Mater.* **1998**, *23*, 295–308.
[15] H. García, S. García, J. Pérez-Prieto, J. Scaiano, *J. Phys. Chem.* **1996**, *100*, 18158–18164.
[16] D. Hay, H. Jaeger, K. Wilshier, *Zeolites* **1990**, *10*, 571–576.
[17] M. Roeffaers, B. Sels, D. Loos, C. Kohl, K. Müllen, P. Jacobs, J. Hofkens, D. De Vos, *ChemPhysChem* **2005**, *6*, 2295–2299.

 © 2007 Wiley-VCH Verlag GmbH & Co. KGaA, Weinheim